2016 American Control Conference (ACC)
Boston Marriott Copley Place
July 6-8, 2016. Boston, MA, USA

A Quantitative Energy and Systems Analysis Framework for Airborne Wind Energy Conversion using Autorotation

Sadaf Mackertich and Tuhin Das

***Abstract*— The principle of autorotation could potentially be utilized for harvesting energy from strong wind fields. Autorotation is a well-known phenomenon where a rotor in a strong wind field experiences significant lift force and aerodynamic torque. With recent works indicating immense, persistent availability of wind energy at high altitudes, autorotation could be used for harvesting wind energy from such altitudes. In this paper, we build upon our previous work and implement a more detailed model of autorotation from one of the seminal works on this topic. The model is computationally challenging but yields steady operating conditions. We enhance this model by incorporating power generation in a manner that is consistent with the governing aerodynamics. This modification helps in quantifying the effects of energy harvesting on the characteristics of autorotation, a study that is not present in the literature. Furthermore, the high spatial resolution of this refined model will help in design-optimization and in control-actuation.**

I. Nomenclature

a	Slope of lift curve for infinite aspect ratio
b	Number of blades
c	Blade chord
W_d	Total weight
I_1	Blade mom. of inertia about flapping hinge
H	Longitudinal force
C_L, C_D	Lift and drag coefficients of blade element
C_T	Rotor thrust coefficient
C_{L_T}	Rotor lift coefficient
C_{D_T}	Rotor drag coefficient
Q	Aerodynamic Torque
R	Blade radius
B	Blade radius fraction less tip losses
T	Thrust force
V	Wind velocity
V_η	Required wind speed for steady autorotation
D	Effective drag force
H	Longitudinal force
L	Effective lift force
θ	Blade pitch angle
α	Angle of incidence
β	Angular rotation of blade about hinge
φ	Angle of oncoming wind at blade element
$a_0, a_1, b_1,$	
a_2, b_2	Fourier series parameters of flapping
α_r	Angle of incidence at blade element
μ	Tip speed ratio
v	Induced axial velocity
λ	Axial flow ratio
ρ	Density of air
σ	Blade solidity
ψ	Angular position of blade
Ω	Angular velocity about shaft
M_W	Flapping moment from blade weight
M_T	Flapping moment from thrust

Sadaf Mackertich is a graduate student and Tuhin Das is an assistant professor of Mechanical and Aerospace Engineering at University of Central Florida, Orlando, FL 32816, Tuhin.Das@ucf.edu

II. Introduction

Wind data from high altitudes shows that there is an abundance of wind power available and that its availability is not restricted by geographical location. Studies in [1] and [2] provide insight into the magnitude of wind power available at altitudes of 7-16km, which is at least an order of magnitude higher than the global energy demand of mankind. This abundance of available energy is primary attributed to global climatic phenomena at higher altitudes, rather than local effects at lower altitudes. A number of designs have been proposed for Airborne Wind Energy (AWE) extraction. A review of these existing designs can be found in [3]. A wind turbine generator mounted on a tethered aerostat was proposed in [4]. Early patents on tethered airborne apparatus for generating energy appear in [5], [6], [7], [8]. In [9], [10], [11], the authors studied kite based energy harvesting devices and proposed the Laddermill, which is a multi-kite AWE system. Additional kite based AWE designs were studied in [12], [13], [14] through modeling, control design and some experiments. Through modeling and simulations, the authors demonstrated energy extraction and analyzed the stability of a tethered-airfoil system connected to a horizontally moving base in [15], [16]. Tethered lighter-than-air aerostats with attached wind turbine(s) are also being investigated, [17], [18]. A few recent studies on AWE systems have advanced to sophisticated automatic control, sensor fusion and performance optimization [19], [20], [21].

The review confirms that current research has exclusively considered tethered AWE devices for relatively low altitudes, $\leq$ 1km. However, by extending the altitude to $\geq$ 5km, one can take advantage of the aforementioned high energy densities. The author's prior research on hot air balloons, [22], has indicated that although a lighter-than-air (LTA) device such as hot air/helium balloon with retrofitted wind turbine(s) may seem pragmatic for simultaneous lift and power generation, a drawback is its lack of maneuverability. The author has also investigated wind energy harvesting using tethered airfoils, [15], [16], where the tether tension is used to mechanically transmit power to the ground. It was concluded that while

978-1-4673-8682-1/$31.00 ©2016 AACC

a tetherd airfoil may be suitable as an AWE device for low altitudes, there are challenges of harvesting energy from high altitudes. In comparison, autorotation have advantages of being maneuverable, producing electricity in-situ, and the ability to switch to powered mode if necessary.

The principle of *autorotation* can be considered in context of the helicopter. While a helicopter generates vertical thrust by accelerating air in the downward direction, autorotation is achieved by placing a freely turning rotor inclined to a wind field. The result is a rotation and an upward thrust, as shown in Fig.1. A rotor undergoing autorotation is termed an *autogyro*. Traditionally, autorotation has been investigated to build gyrocopters [23], or in the context of safe landing of helicopters in case of engine failure, [24], but has not been investigated for wind energy extraction. The blades of an autogyro are free to spin about their common axis, and each blade is additionally free to rotate (flap) about a hinge at its root, which is normal to the spin axis, Fig.1(b). The theory of autorotation can be traced back to the work published in [25]. It uses the BEM (Blade Element Momentum) approach, [26], to model aerodynamic forces. Several works followed [25] to further improve the theoretical basis of autorotation. In particular, in [27], blades with varying pitch were considered to validate against experimental data from Pitcairn-Cierva Autogyro [23], [28], [29]. The work also incorporated a detailed analysis of the forces in the retreating half (see Fig.2(a), (d)), where the blade velocities are reversed. Other extensions include refinement of the analysis of the retreating half for larger angles of attack and higher speeds in [30].

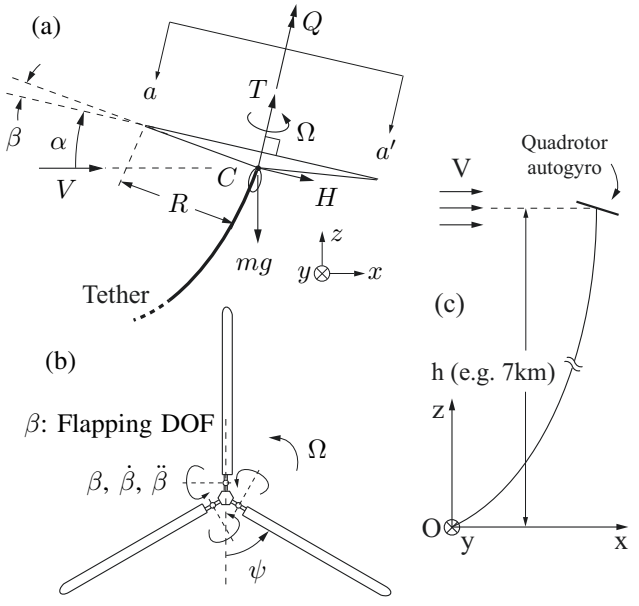

Fig. 1. (a) Forces on an Autogyro [31], (b) View from plane aa' [31], (c) A tethered quadrotor autogyro

In this work, we expand on our previous efforts in [31], which focused on contributions made by Glauert [25], to include further contributions and refinements to the theory by Wheatley [27]. We first provide a summary of the basic theory as established in [25], and then develop the expansion discussed in [27]. Subsequently, we incorporate energy harvesting into the model as a regenerative braking torque and explore the effects of such a torque on the aerodynamics. We provide quantitative results of energy harvested. Finally, we show that spatial distributions of critical aerodynamic parameters over the rotor's disk of rotation, can be derived using the above model. Such distributions can help us pinpoint areas of dynamic stall, predict the distribution of thrust, etc. and thereby provide insight into the overall forcing experienced by a rotor under autorotation.

III. System Description and Simple Model ([25])

Autorotation based AWE harvesting systems could have different configurations. For the sake of simplicity, we consider a tethered autogyro system as shown in Fig.1(c). The system consists of four rotors in a quadrotor configuration, as shown in [31]. Each rotor can either autorotate or be powered. The quadrotor configuration helps maintaining symmetry and stability. It is envisioned that by switching between powered flight and autorotation, the system can maintain attitude and altitude. Electrical power is generated in strong wind fields by using the rotors as generators and is transmitted to ground via the tether. The tether will be heavy but calculations have shown sufficient thrust values that can support its weight. The tether tension will contribute additional forces on the rotor, but in this paper we focus on the aerodynamic characteristics of a single rotor. Tether dynamics and its impacts will be studied in future and will be based on finite-elements or catenary based models, [16].

The model used in [31], based on [25], uses the BEM approach to derive the thrust T, the longitudinal force H, and the rotor torque Q, for a rotor at an angle of incidence α and translating with a speed V. We assumed an inertially fixed rotor in a wind field, with wind velocity V, for which the same analysis is applicable - see Fig.1(a). The analysis assumes that the flapping angle of each blade, β, is a periodic function of the blade's angular position ψ ($\dot{\psi} = \Omega$), and a Fourier expansion is assumed [25], [32], [33], [27]. The flapping angle of each blade is assumed phase-shifted in ψ from the other blades.

In the aforementioned study, expressions of steady-state T, Q, and H are derived under the assumptions that,

1) The angles β and φ are small,
2) The induced axial velocity $v = T/\left(2\pi R^2 \rho V'\right)$, where $V' = \left((V\sin\alpha - v)^2 + V^2\cos^2\alpha\right)^{1/2}$, is constant over the entire span R,
3) The lift coefficient of a blade element is proportional to $\alpha_r = \theta + \varphi$, *i.e.*, $C_L = k\alpha_r$, and the drag coefficient is a constant, $C_D = \delta$.
4) In the Fourier series expansion of the flapping angle β, second and higher harmonics of ψ are negligible, *i.e.*, $\beta = a_0 - a_1\cos\psi - b_1\sin\psi$.

Under the above conditions, the thrust is computed as

$$T = \frac{b}{2\pi}\int_0^{2\pi} d\psi \int_0^R \frac{1}{2}\,\rho\, c\, C_L U^2 dr = T_a \pi R^2 \rho \Omega^2 R^2$$

$$T_a = \sigma\left(\theta + 1.5\lambda\right), \quad \lambda \triangleq \frac{(V\sin\alpha - v)}{\Omega R} \tag{1}$$

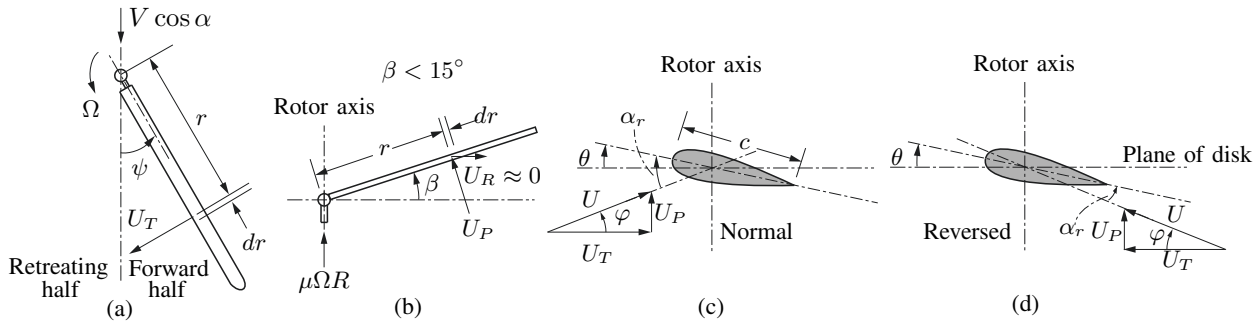

Fig. 2. Blade element views: (a) Along spin axis, (b) Flapping motion, (c) Cross-sectional view, (d) Reversed Velocity Region

where c is the blade chord length, $\sigma \triangleq bcR/(\pi R^2)$ is the solidity ratio, θ is the blade pitch, and λ is the axial speed ratio. The average aerodynamic torque is similarly determined as

$$Q = Q_a \pi R^2 \rho \Omega^2 R^3,\ Q_a = 0.25\sigma\left[\delta - 4\lambda\left(\theta + 1.5\lambda\right)\right] \quad (2)$$

For a desired thrust $T = W_d$, at steady-state the generator torque Q_e (energy harvesting torque) equals the aerodynamic torque Q ($Q = Q_e$), implying

$$\frac{3}{2}W_d R\lambda^2 + \left(W_d R\theta - \frac{3}{2}Q_e\right)\lambda - \left(Q_e\theta + \frac{1}{4}W_d R\delta\right) = 0 \quad (3)$$

$$\Omega = \left[\frac{W_d}{bc\rho R^3\left(\theta + 1.5\lambda\right)}\right]^{1/2} \quad (4)$$

IV. Detailed Model - Model 2: Wheatley [27]

Glauert [25] provided a good basis for the Autogyro theory, but further refinement by Lock [32], [33], followed by Wheatley [27] and then Gessow & Crim [30] provided a more coherent picture and a more reliable model of autorotation. Wheatley's work, built on the work of Lock [32], offered the following refinements:

1) Higher powers of the coefficient of axial velocity λ through disc were evaluated and span-wise variation of induced velocity v was modeled,
2) Higher powers of tip speed ratio μ, where $\mu \triangleq V\cos\alpha/\Omega R$, were included,
3) Blade tip losses and influence of reversed velocities were incorporated, and
4) Span-wise variation of blade pitch was incorporated as a departure from fixed pitch blades.

In addition, [27] also conducted experimental validation of the theory and demonstrated good correlation between theoretical predictions and experiments. On the theoretical side, to incorporate higher order dynamics of the blade's flapping motion, the Fourier series is now expanded to

$$\beta = a_0 - a_1\cos\psi - b_1\sin\psi - a_2\cos 2\psi - b_2\sin 2\psi \quad (5)$$

In subsequent sections, we will discuss the main results of this model and outline steps for numerical computation of aerodynamic variables. The objective of this section is to summarize the existing model of [27] and provide extensions to incorporate into this model the effect of an energy harvesting torque.

A. Thrust Force: T

This section provides the main results related to thrust force calculations in a autogyro under steady autorotation. Variable-pitch blades with a linear change in pitch angle was assumed and the expressions

$$\theta = \theta_0 + \frac{r}{R}\theta_1, \quad \alpha_r = \theta_0 + \frac{r}{R}\theta_1 + \varphi, \quad C_L = a\alpha_r \quad (6)$$

are used as generalization of the fixed pitch analysis. Also, the thrust force was modified to account for tip-speed losses, by defining an effectiveness factor $B \triangleq (1 - 0.5c/R)$, where c is the blade chord length. Further, to incorporate the effects of the reversed velocity region the thrust force formulation of Eq.(1) was modified and essentially split into three different zones, as follows:

$$\begin{aligned} T = {} & \frac{b}{2\pi}\int_0^{\pi} d\psi \int_0^{RB} \frac{1}{2}\rho c a U^2\left(\theta_0 + \frac{r}{R}\theta_1 + \varphi\right) dr \\ & + \frac{b}{2\pi}\int_{\pi}^{2\pi} d\psi \int_{-\mu R\sin\psi}^{RB} \frac{1}{2}\rho c a U^2\left(\theta_0 + \frac{r}{R}\theta_1 + \varphi\right) dr \\ & + \frac{b}{2\pi}\int_{\pi}^{2\pi} d\psi \int_0^{-\mu R\sin\psi} \frac{1}{2}\rho c a U^2\left(-\theta_0 - \frac{r}{R}\theta_1 - \varphi\right) dr \end{aligned} \quad (7)$$

where the elemental velocity components U_T and U_P are $U_T = \Omega r + \mu\Omega R\sin\psi$, $U_P = \lambda\Omega R - r\dot{\beta} - \mu\Omega R\beta\cos\psi$. From the definition of the thrust coefficient

$$C_T \triangleq \frac{T}{\rho\Omega^2\pi R^4}, \quad \sigma = \frac{bc}{\pi R} \quad (8)$$

the following rotor thrust coefficient is obtained

$$\begin{aligned} C_T = {} & \frac{\sigma a}{2}\left\{\frac{\lambda}{2}\left(B^2 + \frac{\mu^2}{2}\right) + \theta_0\left(\frac{1}{3}B^3 + \frac{1}{2}\mu^2 B - \frac{4\mu^3}{9\pi}\right)\right. \\ & \left. + \theta_1\left(\frac{1}{4}B^4 + \frac{1}{4}\mu^2 B^2 - \frac{1}{32}\mu^4\right) + \frac{1}{4}\mu^2 b_2 B + \frac{\mu^3 a_1}{8}\right\} \end{aligned}$$

The rotor lift-coefficient C_{L_T} is given by $C_{L_T} = 2C_T\cos^3\alpha/\mu^2$. In addition, [27] carried out an energy loss analysis to determine the overall rotor drag D. The expression for the D/L ratio, consistent with the order of accuracy (i.e. upto μ^4) is: and the corresponding drag to lift ratio is

$$\frac{D}{L} = \frac{\sigma\delta\left(1 + 3\mu^2 + \frac{3}{8}\mu^4\right)}{8\mu C_T} + \frac{\frac{1}{2}C_T}{\mu(\mu^2 + \lambda^2)^{1/2}}. \quad (9)$$

B. Flapping and Coning Coefficients

The flapping and coning coefficients a_0, a_1, b_1, a_2, and b_2, are critical in all calculations in this model. To solve for these fourier coefficients that define the flapping characteristics, the dynamic equation of flapping $I_1(\ddot{\beta}+\Omega^2\beta) = M_T - M_W$ is used. The reversed velocity region is accounted for in the thrust moment M_T as

$$M_T = \int_0^{RB} \frac{1}{2}\rho c a \left\{ \left(\theta_0 + \frac{r}{R}\theta_1\right) U_T^2 + U_T U_P \right\} r dr \quad (10)$$
$$- 2\int_0^{-\mu R \sin\psi} \frac{1}{2}\rho c a \left\{ \left(\theta_0 + \frac{r}{R}\theta_1\right) U_T^2 + U_T U_P \right\} r dr$$

where the second expression only comes into consideration from $\pi \leq \psi \leq 2\pi$. The equation is expanded using the fourier series expansion of β in Eq.(5). Subsequently, the flapping and coning coefficients are solved by setting the coefficient of each harmonic term, namely constant, $\sin\psi$, $\cos\psi$, $\sin 2\psi$, and $\cos 2\psi$, to zero. The resulting nonlinear simultaneous equations are:

$$a_0 = \frac{\gamma}{2}\left\{ \frac{\lambda B^3}{3} + 0.080\mu^3\lambda + \frac{\theta_0}{4}\left(B^4 + \mu^2 B^2 - \frac{1}{8}\mu^4\right) + \frac{1}{5}\theta_1\left(B^5 + \frac{5}{6}\mu^2 B^3\right) + \frac{1}{8}\mu^2 b_2 B^2 \right\} \quad (11)$$

$$a_1 = \frac{2\mu}{B^4 - \frac{1}{2}\mu^2 B^2}\left\{ \lambda\left(B^2 - \frac{\mu^2}{4}\right) + \frac{4\theta_0 B^3}{3} + 0.106\mu^3\theta_0 + \theta_1 B^4 - \frac{1}{3}b_2 B^3 \right\} \quad (12)$$

$$b_1 = \frac{4\mu B}{B^2 + \frac{1}{2}\mu^2}\left\{ \frac{1}{3}a_0 + \frac{0.035}{B^3}\mu^3 a_0 + \frac{1}{6}a_2 \right\} \quad (13)$$

$$a_2 = \frac{\gamma\mu^2}{144 + \gamma^2 B^8}\left\{ \lambda B\left(16 + \frac{7}{108}\gamma^2 B^8\right) + \theta_0 B^2\left(\frac{46}{3} + \frac{7}{144}\gamma^2 B^8\right) + \theta_1 B^3\left(12 + \frac{7}{180}\gamma^2 B^8\right) \right\} \quad (14)$$

$$b_2 = \frac{-\gamma^2\mu^2}{144 + \gamma^2 B^8}\left\{ \frac{5}{9}\lambda B^5 + \frac{25}{36}\theta_0 B^6 + \frac{8}{15}\theta_1 B^7 \right\} \quad (15)$$

where $\gamma = c\rho a R^4/I_1$ is a nondimensional parameter representing a ratio of aerodynamic to inertia effects in the flapping motion. Wheatley [27] provides a number of simplifications to solve for the fourier coefficients, the details of which the omitted for the sake of brevity.

C. Aerodynamic Torque Incorporating Regenerative Braking

In formulating the aerodynamic torque, this work proposes a modification to [27]. Since the interest of this work lies in energy harvesting, an energy harvesting braking torque Q_e is incorporated in the torque formulation. The average aerodynamic torque is defined in Eq.(2), but upon accounting for the reversed velocity region, blade tip losses, and a generator torque Q_e, the following expression is obtained

$$\frac{4\pi}{b\rho c}Q_e = \int_0^{2\pi} d\psi \int_0^{BR} a\left\{ U_T U_P\left(\theta_0 + \frac{r}{R}\theta_1\right) + U_P^2 \right\} r dr$$
$$- 2\int_\pi^{2\pi} d\psi \int_0^{-\mu R\sin\psi} a\left\{ U_T U_P\left(\theta_0 + \frac{r}{R}\theta_1\right) + U_P^2 \right\} r dr$$
$$- \int_\pi^{2\pi} d\psi \int_0^{R} \delta U_T^2 r dr + 2\int_0^{2\pi} d\psi \int_0^{-\mu R\sin\psi} \delta U_T^2 r dr \quad (16)$$

Neglecting terms large than μ^4, which is consistent with the relaxed assumptions in [27], and rearranging we find

$$\frac{2}{b\rho c\Omega^2 R^4 a}Q_e = \lambda^2\left(\frac{1}{2}B^2 - \frac{1}{4}\mu^2\right) + \lambda\left(\frac{1}{3}\theta_0 B^3 + \frac{2}{9\pi}\mu^3\theta_0 + \frac{1}{4}\theta_1 B^4 + \frac{1}{32}\mu^4\theta_1\right) + \mu\lambda a_1\left(\frac{1}{2}B^2 - \frac{3}{8}\mu^2\right) + a_0^2\left(\frac{1}{4}\mu^2 B^2 - \frac{1}{16}\mu^4\right) - \frac{1}{3}\mu a_0 b_1 B^3 + a_1^2\left(\frac{1}{8}B^4 + \frac{3}{16}\mu^2 B^2\right) + b_1^2\left(\frac{1}{8}B^4 + \frac{1}{16}\mu^2 B^2\right) - a_2\left(\frac{1}{4}\mu^2 a_0 B^2 + \frac{1}{6}\mu b_1 B^3\right) + \frac{1}{2}a_2^2 B^4 + b_2\left(\frac{1}{8}\mu^2\theta_0 B^2 + \frac{1}{12}\mu^2\theta_1 B^3 + \frac{1}{6}\mu a_1 B^3\right) + \frac{1}{2}b_2^2 B^4 - \frac{\delta}{4a}\left(1 + \mu^2 - \frac{1}{8}\mu^4\right) \quad (17)$$

Eq.(17) represents the modified equation for steady-state aerodynamic torque balance, with Q_e representing the energy harvesting torque. In the next section we provide an algorithm for carrying out these computations sequentially or iteratively, for determining steady autorotation conditions in the presence of Q_e.

D. An Algorithm for Computing Steady Autorotation

We provide the following sequence of steps. The first set of steps is suggested when $Q_e = 0$.

(a) Choose a proper range of μ, e.g. $0 < \mu < 0.7$.
(b) Substitute in the physical constants and μ into the flapping coefficient equations Eqs.(11) to (15) and express a_0, a_1, a_2, b_1, b_2 as functions of λ.
(c) Substitute functions from (b) into Eq.(17) and calculate λ. If a no-load operation is of interest, set $Q_e = 0$ and proceed. *If $Q_e \neq 0$, then skip to the iterative algorithm outlined in $1-6$ and then revert back to these steps.*
(d) Substitute λ back into the functions in (b) and retrieve the flapping and coning coefficients.
(e) Utilize λ and μ to calculate values of C_T and α.
(f) Obtain D/L ratio.
(g) Find C_{L_T} and C_{D_T}.
(h) To find the required wind velocity for steady autorotation, set the lift force $L = 0.5 C_{L_T}\rho V_\eta^2 \pi R^2$ equal to the weight W_d and solve for the required wind velocity V_η, which yields $V_\eta = \sqrt{W/(0.5 C_{L_T}\rho\pi R^2)}$.
(i) The steady autorotation speed is $\Omega = V_\eta \cos\alpha/\mu R$.

When a non-zero regenerative torque is added, i.e. $Q_e \neq 0$, we must add a new sequence of steps. This is because now the left hand side of Eq.(17) has the unknown Ω. We first begin with two non-linear equations that are solved simultaneously.

$$\Omega = \sqrt{\frac{W_d}{\rho\pi R^4 C_T(\lambda,\mu)}}, \quad 0 = f(\lambda,\mu) - \frac{2Q_e}{b\rho c\Omega^2 R^4 a} \quad (18)$$

where $f(\lambda,\mu)$ is the right hand side of Eq.(17). Due to the non-linearity of the equations we must solve them iteratively. For a chosen value of μ, Eq.(18) have two unknowns (Ω,λ). We can solve for Ω and λ by following the next sequence of steps:

1) Guess a sufficiently large value of Ω and λ.
2) Substitute Ω and λ into Eqs.(11) through (15) and obtain a_0, a_1, a_2, b_1, b_2.
3) Solve for C_T.
4) Find a new Ω and obtain a new value of λ from Eq.(18).
5) Take new values of Ω and λ and iterate steps (2-5) until solution converges.
6) Repeat the steps (e) to (h) in the first sequence in order to retrieve the new lift coefficients, drag coefficients, and required wind velocity. This allows us to also compute extracted power under a given load Q_e.

V. Simulation Results

To create a basis for understanding the trends, we utilized the parameters defined in [27]. The parameters are listed in Table I. We study aerodynamic conditions and the effect of harvested power. In the plots we superimpose results from [31], which used the Glauert model, [25]. U.S. units were retained in certain results for easier comparison with results in [25], [27]. We first note that the refined model presented

TABLE I
SIMULATION PARAMETERS

Parameter	Value	Description
b	4	Number of blades
R	22.5	Blade radius (ft)
I_1	334	Inertia about flapping hinge slug.ft^2
W_d	3000	Total weight of autogyro (lbs.)
c	1.833	Blade chord (ft)
θ_0	0.0384	Blade pitch at root (rad)
θ_1	1.256×10^{-4}	Slope of blade pitch (rad/in)
K	0.5	Ratio of ν and ν_1
B	$(R-0.5c)/R$	Non-dimensional Constant
a	5.85	Lift curve slope
σ	$Bc/\pi R$	Rotor solidity
δ	0.0120	Mean airfoil drag coefficient
ρ	0.00210	Air density (slugs/ft^3)
γ	$c\rho a R^4/I$	mass constant
Q_e	0-1000	Generator Torque (lb.ft)

in this paper, namely Wheatley, shows similar trends to that of the simplified model, namely Glauert, presented in [31]. This is consistent across all parameters compared, as seen in Fig.3. Another important observation is regarding the implication of the generator torque. Figs.3(a), (b), (c) show steady conditions under $Q_e = 0$, while Figs.3(d), (e), (f) depict the same when $Q_e \neq 0$, i.e. when regenerative braking is present. In all these simulations, operating conditions were determined such that the net lift force would equal or exceed W_d, the weight of the autogyro. We see the a general decrease in all coefficients when $Q \neq 0$, however the required wind velocity V_η only requires minor increase. This is likely due to the 3^{rd} power of V that determines wind power. In general a region of optimum angle of incidence is found around $20^\circ < \alpha < 40^\circ$. In these simulations, the required wind speed appears high. This is primarily because of the high drag coefficient δ used in the simulations. Typically, $0.004 < \delta < 0.008$ is an acceptable range.

The harvested wind power and resulting rotor speeds are plotted in Fig.4(a), (b). The plots are consistent with the expectation that the autorotation speed will reduce as the regenerative torque Q_e increases. The refined model of this paper not only provides more reliable quantitative data but its main advantage is that spatial distribution of aerodynamic parameters such as lift, drag, thrust coefficients can be obtained by removing the spatial averaging done in [27]. A spatial distribution of C_T is shown in Fig.4(c). It is generated by removing the circular and radial averaging of T in Eq.(7) and using the definition of C_T given in Eq.(8). Such resolution shows the regions of the rotor that are favorable and/or unfavorable for producing thrust.

VI. Conclusion and Future Work

Our current work strengthens the idea of using autorotation as a means for extracting wind energy from medium or high altitudes. The existing models of autorotation provide a consistent picture of the phenomenon. Although the models derive steady autorotation conditions, they can provide a strong basis for studies on required actuation and control of optimal operating points. A primary contribution of this work lies in extending the theory of autorotation, which has been traditionally studied for flight, to wind energy applications. This is achieved in this paper by integrating the regenerative braking effect of power extraction into the aerodynamics of the system. Accordingly, steps for numerical deduction of steady operating conditions from the nonlinear system of equations are established. If airborne energy harvesting devices designed on the principle of autorotation are to be realized, the study needs to be further refined by conducting detailed dynamic analysis. Such an analysis will provide a platform for investigating deployment, maneuvering and competitiveness of such devices. This is an ongoing area of research, and preliminary data emerging from the authors' efforts show the usefulness of the above steady autorotation models in constructing dynamic models.

References

[1] B. W. Roberts, D. H. Shepard, K. Caldeira, M. E. Cannon, D. G. Eccles, A. J. Grenier, and J. F. Freidin, "Harnessing high-altitude wind power," *IEEE Transactions on Energy Conversion*, vol. 22, pp. 136–144, 2007.

[2] C. L. Archer and K. Caldeira, "Global assessment of high-altitude wind power," *Energies*, vol. 2, pp. 307–319, 2009.

[3] M. Garcia-Sanz and C. H. Houpis, *Wind Energy Systems: Control Engineering Design*. CRC Press, 2012.

[4] G. Riegler and W. Riedler, "Tethered wind systems for the generation of electricity," *Journal of Solar Energy Enegineering*, vol. 106, pp. 177–181, 1984.

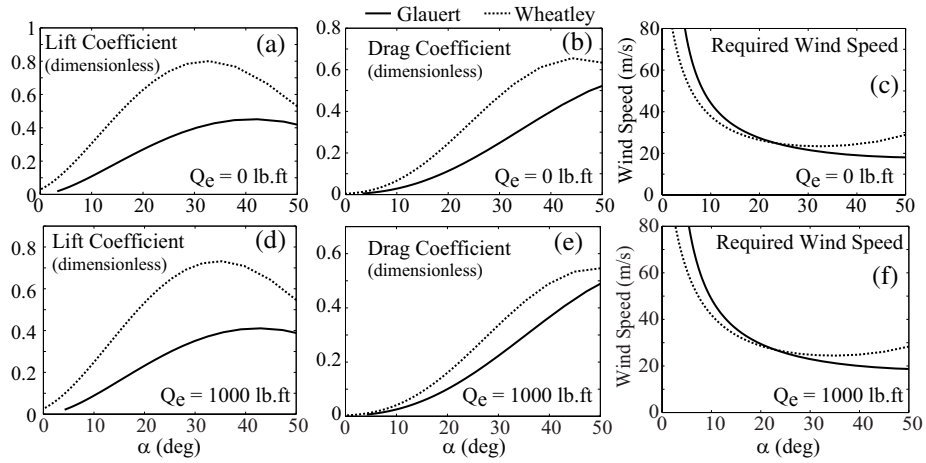

Fig. 3. Impact of Harvesting Wind Energy on the Aerodynamics of Autorotation

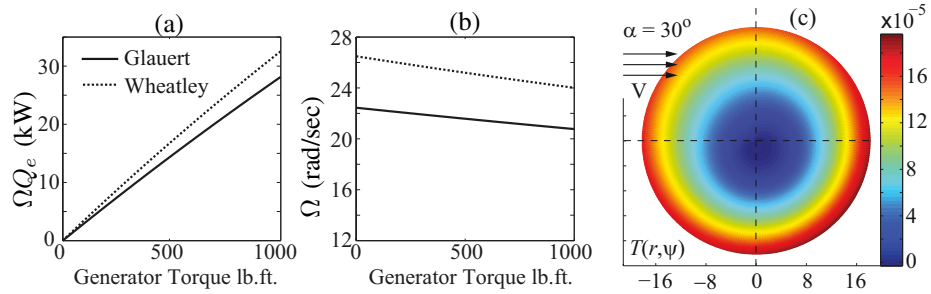

Fig. 4. (a) Power extracted, (b) Steady State Ω needed to maintain required lift, (c) Sample thrust distribution over rotor's disc area

[5] C. M. Fry and H. W. Hise, "Driven high altitude power apparatus," *US Patent 4,084,102*, 1978.

[6] A. Kling, "Wind driven power plant," *US Patent 4,073,516*, 1978.

[7] P. F. Pugh, "Wind generator kite system," *US Patent 4,486,669*, 1984.

[8] L. I. Biscomb, "Tethered airfoil wind energy conversion system," *US Patent 4,309,006*, 1982.

[9] P. Williams, B. Lansdorp, and W. Ockels, "Optimal cross-wind towing and power generation with tethered kites," *AIAA Journal of Guidance, Control and Dynamics*, vol. 31, no. 1, pp. 81–93, 2008.

[10] ——, "Nonlinear control and estimation of a tethered kite in changing wind conditions," *AIAA Journal of Guidance, Control and Dynamics*, vol. 31, no. 3, pp. 793–798, 2008.

[11] W. Ockels, "Laddermill, a novel concept to exploit the energy in the airspace," *Aircraft Design*, vol. 4, pp. 81–97, 2001.

[12] B. Houska and M. Diehl, "Optimal control of towing kites," *IEEE Conference on Decision and Control, San Diego, CA*, 2006.

[13] M. Canale, L. Fagiano, and M. Milanese, "Kitegen: A revolution in wind energy generation," *Energy*, vol. 34, pp. 355–361, 2009.

[14] ——, "High altitude wind energy generation using controlled power kites," *IEEE Transactions on Control Systems Technology*, vol. 18 (2), pp. 279–293, 2010.

[15] T. Das, R. Mukherjee, R. Sridhar, and A. Hellum, "Two dimensional modeling and simulation of a tethered airfoil system for harnessing wind energy," *Proceedings of the ASME Dynamic Systems and Control Conference, Arlington, VA*, 2011.

[16] S. Rimkus, T. Das, and R. Mukherjee, "Stability analysis of a tether-airfoil system," *American Control Conference, Washington DC*, 2013.

[17] N. White, N. Tierno, and M. Garcia-Sanz, "A novel approach to airborne wind energy: Design and modeling," *IEEE Energytech, Cleveland, OH*, May 2011.

[18] C. Vermillion, B. Glass, and A. Rein, "Lighter-than-air wind energy systems," in *Airborne Wind Energy*, U. Ahrens, M. Diehl, and R. Schmehl, Eds. Springer, 2013.

[19] L. Fagiano, A. U. Zgraggen, M. Morari, and M. Khammash, "Automatic crosswind flight of tethered wings for airborne wind energy: Modeling, control design, and experimental results," *IEEE Transactions on Control Systems Technology*, vol. 22, no. 4, pp. 1433–1447, July 2014.

[20] L. Fagiano, K. Huynh, B. Bamieh, and M. Khammash, "On sensor fusion for airborne wind energy systems," *IEEE Transactions on Control Systems Technology*, vol. 22, no. 3, pp. 930–943, May 2014.

[21] S. S. Diwale, I. Lymperopoulos, and C. N. Jones, "Optimization of an airborne wind energy system using constrained gaussian processes," *IEEE Conference on Control Applications (CCA)*, pp. 1394–1399, Oct 2014.

[22] T. Das, R. Mukherjee, and J. Cameron, "Optimal trajectory planning for hot-air balloons in linear wind fields," *AIAA Journal of Guidance, Control, and Dynamics*, vol. 26, no. 3, pp. 416–424, 2003.

[23] B. H. Charnov, *From Autogiro to Gyroplane: The Amazing Survival of an Aviation Technology*. Praeger Publishers, Westport CT, 2003.

[24] J. G. Leishman, *Principles of Helicopter Aerodynamics*. Cambridge University Press, 2000.

[25] H. Glauert, "A general theory of the autogyro," *Presented by the Director of Scientific Research Air Ministry, Reports and Memoranda No. 1111 (Ae. 285)*, 1926.

[26] A. Gessow and G. C. Myers Jr., *Aerodynamics of the Helicopter*. Macmillan Company, New York, 1952.

[27] J. B. Wheatley, "An aerodynamic analysis of the autogiro rotor with a comparison between calculated and experimental results," *National Advisory Committee for Aeronautics, Report No. 487*, 1934.

[28] J. G. Leishman, "Development of the autogiro: A technical perspective," *Journal of Aircraft*, vol. 41, no. 4, pp. 765–781, 2004.

[29] "Gyrocopter vs helicopter," http://www.phenix.aero/PHE-1210.html, 2013.

[30] A. Gessow and A. D. Crim, "An extension of lifting rotor theory to cover operations at large angles of attack and high inflow conditions," *National Advisory Committee for Aeronautics, Technical Note No. 2665*, 1952.

[31] S. Rimkus and T. Das, "An application of the autogyro theory to airborne wind energy extraction," *ASME Dynamic Systems and Control Conference (DSCC), Palo Alto, CA*, October, 2013.

[32] C. N. H. Lock, "Further development of autogyro theory - part i," *National Advisory Committee for Aeronautics, Reports and Memoranda No. 1127 (Ae. 299)*, 1927.

[33] ——, "Further development of autogyro theory - part ii: A general treatment of the flapping motion," *National Advisory Committee for Aeronautics, Reports and Memoranda No. 1127 (Ae. 299)*, 1927.